How the combination of electromagnetic effects and thermophysical properties of solids influences the formation of laser induced periodic surface structures

GEORGE D. TSIBIDIS[1,2*] , PANAGIOTIS LINGOS[1] , EMMANUEL STRATAKIS[1,3]

[1]Institute of Electronic Structure and Laser (IESL), Foundation for Research and Technology (FORTH), Vassilika Vouton, 70013, Heraklion, Crete, Greece

[2]Department of Materials Science and Technology, University of Crete, 71003, Heraklion, Greece

[3]Department of Physics, University of Crete, 71003, Heraklion, Greece

*tsibidis@iesl.forth.gr

ABSTRACT

To realize efficient material processing and account for the formation of laser induced periodic surfaces structures (LIPSS), it is very important to understand the fundamental laser-matter interaction processes. In this work, we follow a systematic approach to predict the *pulse-by-pulse* formation of LIPSS on metals due to the development of a spatially periodic energy deposition that results from the interference of electromagnetic far fields on a non-flat surface profile. We demonstrate that the induced electromagnetic effects, alone, are not sufficient to allow the LIPSS formation, therefore, we emphasize on the crucial role of electron diffusion and electron-phonon coupling on the formation of stable periodic structures. Gold and stainless Steel are used as two materials to test the model.

1. INTRODUCTION

The employment of femtosecond (fs) pulsed laser sources for material processing has received significant attention due to the important technological applications [1]. Various types of surface nano/micro-structured topographies have been fabricated by exploiting the wealth of possibilities laser technology offers through modulation of the laser parameters [1,2].

Despite the presence of several theoretical frameworks that aim to elucidate the surface modification related underlying physical processes, it has been postulated that the pattern formation is attributed to a great extent to the response of the solid to the electromagnetic radiation [1,3,4]. However, experimental results for various metals showed that while the size and origin of the periodicity of LIPSS can be ascribed to electromagnetic effects, the manifestation of the depth profile of the produced periodic structures varies [5,6]. Although, one might argue that, the electromagnetic response of the irradiated material (i.e. different extinction coefficient) accounts for this behavior, experimental observations demonstrate that other physical mechanisms can potentially be involved that allow or inhibit the formation of distinct periodic structure.

In this work [4], we demonstrate that the thermophysical properties of the material themselves play a crucial role in the formation of periodic patterns. To this end, we have conducted a multiscale physical modelling approach to describe pattern formation on two materials, gold (Au) and stainless Steel (SS) that are characterized from distinctly different thermophysical properties.

2. THEORETICAL PREDICTIONS

Our theoretical predictions are aimed to reveal the significant role of the differences in the electron

diffusion and electro-phonon coupling strengths in the two materials to the features of the induced topographies. We emphasize the interplay between the electromagnetic and thermophysical properties in the produced amplitude of periodic structures through a detailed theoretical investigation. In our simulations, linearly polarized laser beams of pulse duration 170 fs (FWHM) were used. It is noted that the electric field is polarized along the *X*-axis.

To describe, firstly, the electromagnetic response of the two materials, lightly rough surfaces are assumed. The aim is to show that non-flat topographies account for the excitation of electromagnetic modes that are precursors of periodic structures. To emulate the rough patterns, a configuration of a random distribution of sub-wavelength hemispherical holes (radius randomly ranged between $10< R < 100$ nm) is used along the surface. A similar approach has been introduced in previous reports [3].

The interaction of light with the surface inhomogeneities of the material produces electromagnetic interference patterns along the surface which determines the energy absorption landscape. Hence, the investigation of the periodic (or quasi-periodic) electromagnetic modes along the surface is the first step in our multi-physical study. The interference between the incident light beam with the scattered waves generated by surface nano-defects on metallic surfaces as a result of dipole-dipole coupling, produce standing mixed waves such as Surface Plasmon Polaritons (SPP) and quasi-cylindrical evanescent waves [3]. The optical properties of the irradiated material determine the characteristics of these waves such as scattering, absorption, transmission, the optical propagation length as well as the skin depth. To reveal the electromagnetic response of the material, a Finite Integration Technique is employed for the solution of the full-vector 3D Maxwell-Grid Equations [4]. Assuming a laser beam at a fixed wavelength $\lambda_L = 513$ nm, the dielectric constants considered in the simulations are $\varepsilon_{Au} = -3.43 + i3.01$ and $\varepsilon_{SS} = -0.45 + i16.3$ for Au and SS, respectively, whereas the hemispherical nano-holes are assumed to be filled with air ($\varepsilon = 1$).The electric field of the laser beam is presented as a plane-wave linearly polarized along the X-axis arriving at normal incidence to the surface. The geometry of the problem allows to use a simple representation of the boundary conditions and the computational grid is terminated by two convolutional perfectly matched layers (convPML) [4] along the *Z*-direction to avoid non-physical reflections while periodic boundary conditions are used for *X* and *Y* directions.

It is noted that in order to compare the surface deformation of both materials following the multi-pulse irradiation, we used identical surface topographies before the arrival of the initial laser pulse. To acquire information about the energy absorption in these two samples, we illustrated the inhomogeneous distribution of the intensity, $I \sim \left|\vec{E}\right|^2$ (where $\vec{E}$ stands for the electric field), below the rough surface normalized with respect to the maximum intensity of the flat surface I_S or the maximum intensity of the incident beam by the source. In Fig.1a-b, we show the normalized intensity difference $(I - I_S)/I_S$ below the surface in the transverse plane perpendicular to light wave-vector, which depicts the intensity maxima and minima due to both scattered radiative and non-radiative fields by the subwavelength imperfection. It appears, that the presence of the nano-holes in the metallic surfaces favor the energy deposition at their edges, localized parallel to the laser polarization, while the far fields consisting of SPP and quasi-cylindrical wave components exhibit maxima and minima that are formed perpendicularly to the laser polarization. For both metals in the current work, the superposition of the incident beam with the scattered far fields determines the energy absorption maps along the surface. It is noted that there exists a strong difference in the optical properties and response of the materials: (a) the absorption coefficient (b) the SPP propagation length and (c) the skin depth. For instance, the absorption coefficient of is $a_{Au} = 81.73\ \mu\text{m}^{-1}$ and $a_{SS} = 47.75\ \mu\text{m}^{-1}$ for the two materials. The SPP propagation length is $L_{Au} \approx 100\ \mu$m for Au and $L_{SS} = 0.23\ \mu$m for SS. Despite these differences, the absorption features of these materials are quite similar and they are determined by the radiative far fields. On the other hand, the near field couplings are negligible because the average distance between the nano-holes is nearly equal to the laser wavelength. As a result, the periodic/quasi-periodic absorption features are observed with average periodicity $\approx \lambda_L$. This is also captured in Fast Fourier Transforms of the corresponding absorption maps ($k_x/k_0 \approx \pm 1$) (Fig.1c-d). Moreover, the periodic absorption features are strongly defined by the SPP. In Fig.1e-f, we present the normalized *Z*-component of the electric

field at the propagation plane *XZ* which depicts the SPP along the air-metal interface; in the case of Au, the SPP is pronounced compared to the stainless steel. To correlate the

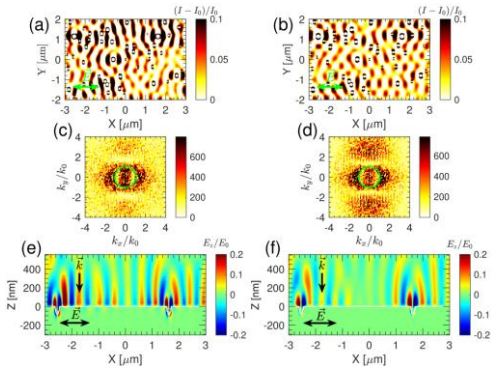

Fig.1. Absorbed energy distributions on the transverse plane for Au (a) and SS (b) surfaces (*NP*=1). (c), (d) illustrate the Fourier transform of (a), (b), respectively. The *green* circles represent the boundary of $|k| = k_0$ where $k_0 = 2\pi/\lambda_L$ stands for the wave-vector of light propagation in air (double headed arrow indicates laser polarization direction). (e) and (f) illustrate normalized *Z*-component of the electric field at the propagation plane *XZ*. In this cross section, two nano-holes are located at positions *X*=-2540 nm and *X*=1630 nm. The *white* line represents the air-metal interface.

electromagnetic response of the material with changes occurring along the irradiated surface in a pulse after pulse approach, a side view of the distribution of the absorbed energy is illustrated for both materials on the *XZ* plane (the propagation plane) for four pulses (*NP*=4) (Fig.2a and Fig.2b); by contrast, results illustrated in Fig.1 are obtained for *NP*=1. The electric field (*Z*-component) distribution on the propagation plane for the two materials is also illustrated in Fig. 2c and Fig.2d. Results for Au and SS demonstrate similar far field interference patterns of the absorbed energy, following scattering of the electromagnetic fields off the hole scatterers. The quasi-periodic interference patterns (Fig.1a,b) induced by nanoscale surface imperfections can explain the formation mechanism of laser-induced patterns [3,4]. Thus, a reasonable outcome of such electromagnetic field distribution would be the formation of periodic structures (LSFL) on the surface of both materials. Nevertheless, experimental results indicate that, unlike in SS, the amplitude of the ripples formed on bulk Au is very small even at very large number of pulses [6]. This outcome suggests that other effects related to the properties of the metals and thermal response of system after absorbing the laser energy might account for the distinct differences.

To describe the process towards pattern formation we use a theoretical model that comprises a Two Temperature Model (TTM) coupled with a Navier-Stokes equation that provides a detailed analysis of the fluid dynamics [2,4]. Due to the large electron heat diffusion and ballistic transport for Au, less energetic electrons remain on the surface of the material to couple with the lattice system. By contrast, the behavior of SS, both in terms of electron diffusion and electron-phonon coupling strength, is different: the electron heat conductivity length is four times smaller than those for Au while the electron phonon coupling strength is ten time stronger and it follows a decreasing monotonicity with increasing electron temperature (opposite to that of Au). As a result, larger lattice temperatures are confined in a smaller region, thus the developed temperature gradients are more enhanced and finally, the induced hydrothermal waves will have larger amplitudes, giving rise to pronounced periodic profiles upon resolidification [4].

To illustrate the effect of repetitive irradiation, we have carried out simulations at increasing *NP*. Results show an enhanced absorption in the wells of the periodic profile (Fig.2). As repetitive irradiation is expected to increase the amplitude of the induced periodic structures due to mass transport, the theoretical framework was applied to predict the variation of the height and periodicity of the ripples (Fig.3). Simulations results for both Au and SS show a shallow ripple profile for Au (Fig.3a), compared to higher ripple amplitudes for SS (Fig.3b) due to the predominantly energy confinement for SS. Although simulations shown in Fig.3 provide results for *NP*=4, similar conclusions can be deduced at higher *NP*. With respect to the periodicity variation at increasing *NP*, it

is noted that results in previous works showed a decrease of the ripple periodicity as *NP* increases [2,3]; by contrast, our simulations indicate that for a small *NP*, an apparent ripple periodicity reduction is not predicted (Fig.3c). Finally,

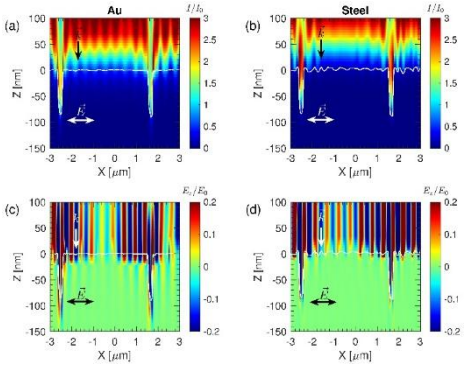

Fig.2. Absorbed energy distributions on the propagation plane for (a) Au and (b) SS surfaces (*NP*=4). Electric field (*Z*-component) distribution for Au (c), SS (d). The *white* line defines the boundary of the surface profile along the air-metal interface.

the expected increase of the amplitude of the produced ripples for SS, in contrast to Au, at increasing *NP* is illustrated in Fig.3d.

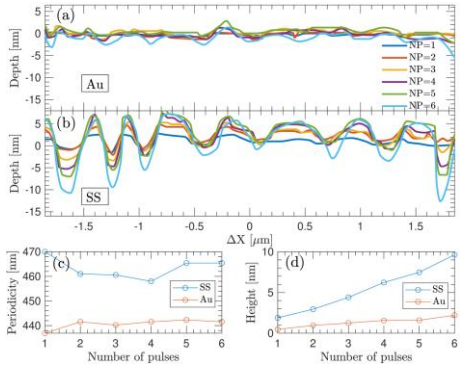

Fig.3. Amplitude of LIPSS as a function of number of pulses for (a) Au and (b) Stainless steel. Average periodicity (c) and (d) amplitude of LIPSS *vs* number of pulses.

3. CONCLUSIONS

Our approach was aimed to interpret the differences in the periodic pattern amplitudes following irradiation of materials with distinctly different thermophysical properties. The investigation (i) predicts the excitation of electromagnetic modes of periodicities of the size of the wavelength, and (ii) demonstrates the significant influence of the electron diffusion and electron-phonon coupling on the features of the expected periodic patterns. While, in the current study, the focus is on the LSFL features on Au and SS, a similar approach could be followed for other materials.

Funding. *BioCombs4Nanofibres* (grant agreement No. 862016); *NEP* project (GA 101007417); COST Action *TUMIEE*.

REFERENCES

[1] E. Stratakis *et al.*, Materials Science and Engineering: R: Reports **141**, 100562 (2020).
[2] G. D. Tsibidis, M. Barberoglou, P. A. Loukakos, E. Stratakis, and C. Fotakis, Physical Review B **86**, 115316 (2012).
[3] A. Rudenko, C. Mauclair, F. Garrelie, R. Stoian, and J. P. Colombier, Applied Surface Science **470**, 228 (2019).
[4] G. Tsibidis, P.Lingos, and E. Stratakis, Optics Letters **47**, 4251 (2022).

[5] J. C. Wang and C. L. Guo, Applied Physics Letters **87**, 251914 (2005).
[6] F. Fraggelakis, G. D. Tsibidis, and E. Stratakis, Physical Review B **103**, 054105 (2021).